Organic Electronics 13 (2012) 13–17

Contents lists available at SciVerse ScienceDirect

Organic Electronics

journal homepage: www.elsevier.com/locate/orgel

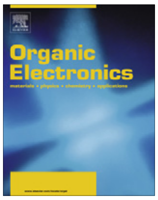

Correlations of impedance–voltage characteristics and carrier mobility in organic light emitting diodes

I-Wen Wu, Po-Sheng Wang, Wei-Hsuan Tseng, Jung-Hung Chang, Chih-I Wu *

Graduate Institute of Photonics and Optoelectronics and Department of Electrical Engineering, National Taiwan University, Taipei 106, Taiwan

ARTICLE INFO

Article history:
Received 16 May 2011
Received in revised form 16 September 2011
Accepted 18 September 2011
Available online 14 October 2011

Keywords:
OLED
Mobility
Impedance

ABSTRACT

The correlation of accumulation charges at the interfaces of organic layers and carrier mobility in organic light emitting devices (OLEDs) were investigated through the impedance versus voltage (*Z*–*V*) characteristics of devices. The properties of devices with various combinations of cathode structures, HTLs and ETLs were investigated to understand the impedance transition in *Z*–*V* characteristics of OLEDs. It was observed that there is an extra impedance transition before devices turn on when the hole mobility in the HTL is much greater than the electron mobility in the ETL in the devices, which makes the *Z*–*V* characteristics a potential tool to compare the electron mobility in ETL and hole mobility in HTL.

1. Introduction

The current density versus voltage (*J*–*V*) and luminescence versus voltage (*L*–*V*) measurements are widely-used methods to evaluate and describe the performance of an organic light emitting diode (OLED). They directly show the cumulative results of the carrier injection, carrier transport, carrier recombination, and the light radiation. However, both of the *J*–*V* and *L*–*V* characteristics can reveal the behavior of the devices only when the devices start to conduct current and they provide little information of devices under reverse bias. The impedance versus voltage (*Z*–*V*) measurement is another way to investigate the electrical properties of OLED devices. Most importantly, it can be used to study the characteristics of device even before the current flow through the devices. For instance, Brütting et al. had demonstrated the existence of the accumulation charges at the organic layers interfaces through the impedance transition in *Z*–*V* characteristics of OLEDs [1–3]. In this work, the correlation between the impedance behaviors in *Z*–*V* characteristics and the devices with various cathode structures and the organic materials, as the electron transport layers (ETLs) or the hole transport layers (HTLs), was systematically investigated. The results revealed that the occurrence of the extra impedance transition is correlated to the difference between the hole mobility in HTLs and the electron mobility in ETLs. Therefore the *Z*–*V* characteristics can be used to find out the relation of the carrier mobilities in two carrier transport layers and to estimate the carrier mobility for new organic materials. There have been several methods developed to measure the carrier mobility in semiconductors or organic materials. For instance, the time of flight (TOF) method calculates the carrier mobility in materials by measuring the time the carriers need to travel a certain distance across the material [4–6]. This method is also quite simple and straightforward. But in order to eliminate the deviation caused by the measurement limits, its application is restricted to thick films, which would consume lots of materials and is therefore not suitable for rare and precious materials. Another common method is the transient electroluminescence (TREL), in which one could apply a voltage pulse to devices and estimate the carrier mobility by the delay time of the EL signal [7–9]. The accuracy of this method

---

* Corresponding author.
E-mail address: chihiwu@cc.ee.ntu.edu.tw (C.-I. Wu).

1566-1199/$ - see front matter © 2011 Elsevier B.V. All rights reserved.
doi:10.1016/j.orgel.2011.09.016

may be influenced by the RC delay of the circuits or by the errors from identifying the start of the EL signal. There are other techniques can be applied to extract the carrier mobility of organic materials, such as dark-injection space-charge-limited-current (DI SCLC), space charge limited current (SCLC) [10], and admittance spectroscopy (AS) [11]. The DI SCLC and SCLC methods are developed based on some carrier transport theory and estimate carrier mobility through numerical fitting or analyzing the current density versus voltage characteristics. As for the AS analysis, it extracts the carrier mobility by the plot of the computer-simulated negative differential susceptance versus frequency. Compared with these present methods, the *Z–V* characteristics method in this work is relatively simple and material-saving and does not need complex numerical fitting or analysis, which can be used as a more intuitive and uncomplicated alternative to preliminarily evaluate the carrier mobility.

2. Experiments

All the investigated OLED devices were fabricated on glass substrates pre-coated with a high work function ITO anode of 120 nm thick. Before the fabrication process, the substrates were cleaned by detergent, acetone, and methanol in ultrasonic bath for 10 min sequentially and treated by UV ozone for 10 min to remove the particles on the surface and increase the work function. The organic layers, including hole transport layers, electron transport layers, and electron injection layers, and the patterned cathodes were deposited in a thermal evaporation chamber equipped with up to eight sublimation sources. During the deposition of each layer, the base pressure of the chamber was about 10^{-6} torr and the temperature was maintained by the water cooling system. The deposition rate and the accumulated thickness were monitored by quartz crystals which have been calibrated by the surface profiler. The sample holder and mask holder in evaporation chamber allowed altering masks in-situ and rotating sample during deposition to eliminate the contamination of ambient and to provide more uniformly deposited films. The organic materials used in this study include N,N′-di(naphthalene-1-yl)-N,N′-diphenylbenzidine (NPB) and N,N′-diphenyl-N,N′-bis(3-methylphenyl)-[1,1′-biphenyl]-4,4′-diamine (TPD) as HTLs and Tris(8-hydroxyquinoline) aluminum (Alq_3), 4,7-diphenyl-1,10-phenanthroline (BPhen), 2,9-Dimethyl-4,7-diphenyl-1,10-phenanthroline (BCP), and 2,2,2-(1,3,5-benzenetriyl)tris-[1-phenyl-1H-benzimidazole] (TPBI) as ETLs.

The current density–voltage (*J–V*) characteristics were measured by a Keithley 2400 source meter. The impedance–voltage (*Z–V*) and phase-voltage characteristics were evaluated by an Agilent E4980A LCR meter, with a sinusoidal signal of 0.1 V amplitude and 100 Hz frequency. The phase-voltage characteristics were also measured to investigate the electrical properties of the devices under different voltage bias, in which the 0° phase indicates the conductive state and the −90° represents for the insulating phase.

3. Results and discussion

First, the devices with identical organic layers but various cathode structures were fabricated to investigate the correlation between the *Z–V* characteristics and the electron injection efficiency. The *J–V* and *Z–V*, and phase-*V* characteristics of devices with NPB as a HTL, Alq_3 as an ETL, and various cathode structures, including Al, Mg, and LiF/Al, were shown in Fig. 1. The *J–V* curves in Fig. 1a show that the turn-on voltages, which are defined at the voltage when the current drastically increases, of these devices are exactly the same. As for the *Z–V* and phase-*V* characteristics shown in Fig. 1b and c, there are two transitions in each *Z–V* curves, one occurs at lower voltages before the turn-on indicating the existence of the accumulation charges [1,2], and the other falls at the same voltage where the phase ascends. The sharp rise of the phase associated with the second impedance transition indicates the turn-on voltage of the device, which agrees with the result from the *J–V* characteristics. Before the devices turn on, the impedance transition voltages and the ratios of the

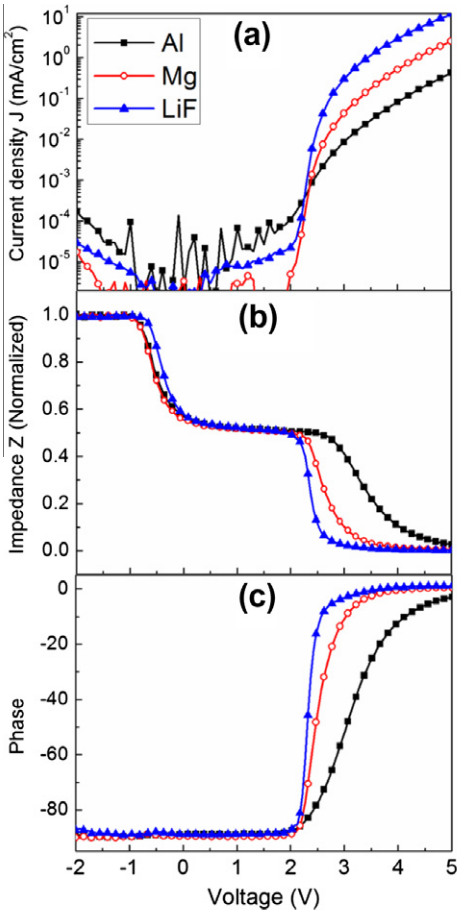

Fig. 1. The (a) current density versus voltage (*J–V*), (b) impedance versus voltage (*Z–V*), and (c) phase versus voltage characteristics of OLEDs with different cathode structures. The film structures of these devices are as follows. (1) Al: ITO/NPB(800 Å)/Alq_3(800 Å)/Al, (2) Mg: ITO/NPB(800 Å)/Alq_3(800 Å)/Mg, (3) LiF: ITO/NPB(800 Å)/Alq_3(800 Å)/LiF/Al.

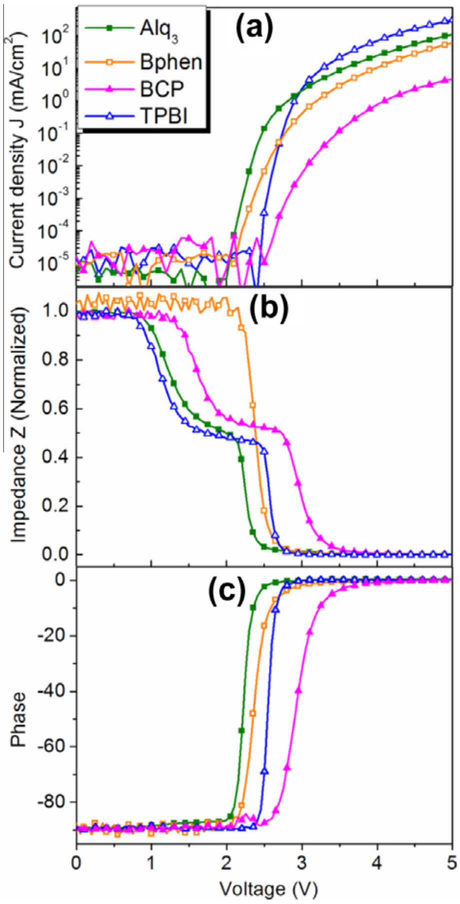

Fig. 2. The (a) current density versus voltage (*J*–*V*), (b) impedance versus voltage (*Z*–*V*) and (c) phase versus voltage characteristics of OLEDs with various ETLs. The film structures of these devices are shown as follows: (1) Alq_3: ITO/NPB(400 Å)/Alq_3(400 Å)/LiF/Al, (2) BPhen: ITO/NPB(400 Å)/BPhen(400 Å)/LiF/Al, (3) BCP: ITO/NPB(400 Å)/BCP(400 Å)/LiF/Al, (4) TPBI: ITO/NPB(400 Å)/TPBI(400 Å)/LiF/Al.

impedance drop after transition are quite similar. The results verify that the accumulation charges at the organic layer interfaces are independent on the cathode structures and the electron injection of the devices.

Another issue is whether the existence of the accumulation charges at the organic layer interfaces only occurs at certain ETL–HTL combinations. To examine the dependency of the accumulation charges on organic materials, experiments were implemented on devices with several kinds of ETLs, such as Alq_3, BPhen, BCP and TPBI. All these devices were built on ITO substrates as anodes with NPB as HTLs and LiF/Al as cathodes. Similarly, the *J*–*V*, *Z*–*V*, and phase-*V* characteristics of these devices were analyzed and plotted in Fig. 2. The turn-on voltages of the devices, shown in Fig. 2a and c, are varied with different ETLs and are corresponding to the energy differences of ETL's LUMOs and HTL's HOMOs at the interfaces [12]. In Fig. 2b, there is an extra impedance transition at around 1 V before devices turn on in *Z*–*V* characteristics of the devices with Alq_3, BCP, TPBI as ETLs, but no such a transition exists in *Z*–*V* characteristics of the device with BPhen as an ETL. The carrier mobilities in these materials are listed in Table 1 [13–16] and it reveals an interesting dependency of impedance transition on the difference between carrier mobilities of NPB (HTL) and ETLs. In the devices with electron mobility of ETLs much smaller than the hole mobility of the HTL, there is an extra impedance transition before device turns on in *Z*–*V* characteristics. But there is no such impedance transition in devices with electron mobility of ETLs similar to the hole mobility of the HTL.

Table 1
The carrier mobilities of organic materials used as ETLs and HTLs.

ETL materials	Alq_3	BPhen	BCP	TPBI
Electron mobility	1.4×10^{-6}	3.9×10^{-4}	6×10^{-7}	3.3×10^{-5}
HTL materials	NPB	TPD	Units	
Hole mobility	5×10^{-4}	1×10^{-3}	$cm^2/V\ s$	

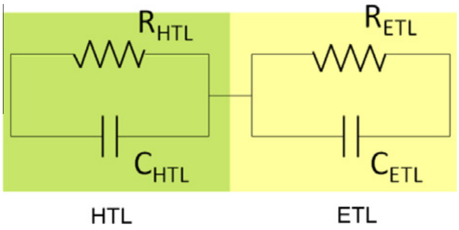

Fig. 3. The equivalent circuit of hole transport layer (HTL) and electron transport layer (ETL) in OLEDs.

According to the previous study of Brütting et al. [1,2], in the presence of the accumulation charges, an electric field difference occurs between two carrier transport layers and only one of the organic layers reaches flat band first before devices turn on, leading to an extra impedance transition in the *Z*–*V* characteristics in addition to the transition at the turn-on voltage. The equivalent circuit of the organic layers with HTLs and ETLs can be expressed as Fig. 3. Under reverse bias, both of the organic layers behave like capacitors with large resistances. As the voltage bias increases to a certain value, one of the organic layers might become more conductive, resulting in the decrease of the total impedance of the whole device. Finally, after the device turns on, both organic layers are conductive and the impedance approaches zero. This equivalent circuit explains for the correlation of the carrier mobilities in electron and hole transport layers and the device behavior in *Z*–*V* characteristics. If the hole mobility in HTL is much larger than the electron mobility in ETL, the unbalance of the electron and hole transports in organic layers might lead to the accumulation charge at the organic–organic interfaces and in such as case the HTL will become conductive first before the device turns on, which results in the existence of the extra impedance transition at lower bias.

To further verify this inference, the organic material TPD which has larger hole mobility than that of NPB was chosen as an HTL. The *J*–*V*, *Z*–*V* and phase-*V* characteristics of devices with combinations of NPB and TPD as HTLs and Alq_3 and BPhen as ETLs are shown in Fig. 4. There is an

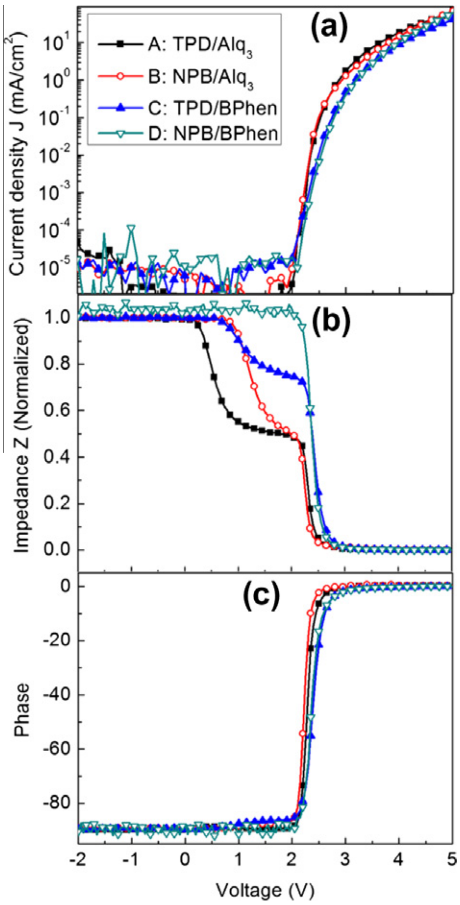

Fig. 4. The (a) current density versus voltage (*J*–*V*), (b) impedance versus voltage (*Z*–*V*), and (c) phase versus voltage characteristics of OLEDs with various HTLs and ETLs combinations. The film structures of these devices are shown as follows: (1) A: ITO/TPD(400 Å)/Alq_3(400 Å)/LiF/Al, (2) B: ITO/NPB(400 Å)/Alq_3(400 Å)/LiF/Al, (3) C: ITO/TPD(400Å)/BPhen(400Å)/LiF/Al, (4) D: ITO/NPB(400 Å)/BPhen(400 Å)/LiF/Al.

extra impedance transition before devices turn on in *Z*–*V* characteristics of the devices with NPB/Alq_3, TPD/Alq_3 and TPD/Bphen as HTLs/ETLs, respectively. But only one transition at the turn-on voltage is found in *Z*–*V* characteristics of the device with NPB/BPhen as the HTL/ETL, shown as Device D in Fig. 4b. From the carrier mobility of organic materials listed in Table 1, Device D, with NPB/BPhen as the HTL/ETL, is the only device which has electron mobility in ETL comparable to the hole mobility in HTL. These results indicate that the extra impedance transition would exist in the devices with the hole mobility in the HTL much greater than the electron mobility in the ETL, while it is not found in the devices with similar hole and electron mobility in the HTL and the ETL, respectively. It is suggested that the accumulation charges are related to the huge different mobilities of hole and electron in HTL and ETL, respectively. This is because that when the resistance of the ETL is much larger than that of the HTL, it can provide the electric field difference between the HTL and the ETL, which makes the HTL reach flat band before the device turns on.

Since the occurrence of the impedance transition is dependent on the difference between the carrier mobilities in the HTL and ETL, the *Z*–*V* characteristics have the potential to be used as a preliminary tool to investigate the relation between the hole and electron mobilities in two organic materials. The magnitude of the carrier mobility in hole or electron transport organic materials can be roughly evaluated by the *Z*–*V* characteristics of devices with simple HTL/ETL bilayer structures if one of the carrier mobilities in either HTL or ETL is known. The *Z*–*V* characteristics of this simple device would distinguish whether the electron mobility in the ETL is close to the hole mobility in the HTL. Using *Z*–*V* characteristics to estimate the mobility, the required film structures of the devices are very simple and do not need a huge amount of organic materials for the testing, such as in the TOF measurement. The experimental data does not need to be fitted or dealt with any numerical calculation, and this method is still applicable for the organic materials with low emission efficiency or even non-emissive materials. However, instead of measuring the accurate value of the carrier mobility, the *Z*–*V* characteristics can only reveal whether the hole and electron mobilities in the carrier transport layers are comparable. Even though the *Z*–*V* characteristics can only be used to roughly estimate the order of magnitudes of carrier mobilities, it is a convenient method to make a quick-turn evaluation of the carrier mobility.

It is important to note the limitation of using *Z*–*V* characteristics to estimate the carrier mobility. The impedance characteristic method described in this report can be used to analyze the relation between the hole and electron mobility in the carrier transport layers. It can distinguish whether or not the electron mobility in the ETL is comparable to the hole mobility in the HTL. To estimate the electron mobility in an organic material, a list of known HTLs with a wide range of hole mobilities is needed. Then the devices with the tested ETL and several known HTLs should be investigated to compare the electron mobility with the hole mobility in each HTLs. The result of these comparisons would show the range of the electron mobility of the tested material. However, the accuracy is still limited to one order or worse.

4. Conclusion

The correlation between the *Z*–*V* characteristics and the carrier mobilities of the electron transport and hole transport materials in OLEDs was investigated. For the devices with same HTLs and ETLs, the transitions of the impedance in the *Z*–*V* characteristic are almost the same regardless of the cathode structures. The *Z*–*V* characteristics of the devices with various combinations of HTLs and ETLs were also examined. In all the devices investigated, there is an extra impedance transition occurred at the lower voltages before the turn-on voltage in the devices with the hole mobility in the HTL much larger than the electron mobility in the ETL. Thus it is suggested that the large different carrier mobilities would result in the existence of the accumulation charges at the organic interfaces. Therefore the *Z*–*V* characteristics can provide information about the carrier mobility in the carrier transport layers and can be used as a potential tool to roughly estimate the carrier mobility in new organic materials.

Acknowledgment

This work was partially supported by National Science Council, the Republic of China under Contract Nos. NSC 98-2112-M-002-016 and NSC 100-3113-E-002-012.

References

[1] S. Berleb, W. Brütting, G. Paasch, Org. Electron. 1 (2000) 41.
[2] W. Brütting, S. Berleb, A.G. Mückl, Org. Electron. 2 (2001) 1.
[3] W. Riess, H. Riel, T. Beierlein, W. Brütting, P. Müller, P.F. Seidler, IBM J. Res. Dev. 45 (1) (2001) 77.
[4] I.H. Campbell, D.L. Smith, C.J. Neef, J.P. Ferraris, Appl. Phys. Lett. 74 (1999) 2809.
[5] W.Y. Hung, T.H. Ke, Y.T. Lin, C.C. Wu, T.H. Hung, T.C. Chao, K.T. Wong, C.I. Wu, Appl. Phys. Lett. 88 (2006) 064102.
[6] A.J. Campbell, D.D.C. Bradley, H. Antoniadis, Appl. Phys. Lett. 79 (2001) 2134.
[7] S.C. Tse, H.H. Fong, S.K. So, J. Appl. Phys. 94 (2003) 2034.
[8] Z.Y. Xie, T.C. Wong, L.S. Hung, S.T. Lee, Appl. Phys. Lett. 80 (2002) 1478.
[9] M. Ichikawa, J. Amagai, Y. Horiba, T. Koyama, Y. Taniguchi, J. Appl. Phys. 94 (2003) 7796.
[10] D. Poplavskyy, J. Nelson, J. Appl. Phys. 93 (2003) 341.
[11] S.W. Tsang, S.K. So, J.B. Xu, J. Appl. Phys. 99 (2006) 013706.
[12] I.W. Wu, Y.H. Chen, P.S. Wang, C.G. Wang, S.H. Hsu, C.I. Wu, Appl. Phys. Lett. 96 (2010) 013301.
[13] S.C. Tse, K.C. Kwok, S.K. So, Appl. Phys. Lett. 89 (2006) 262102.
[14] R.G. Kepler, P.M. Beeson, S.J. Jacobs, R.A. Anderson, M.B. Sinclair, V.S. Valencia, P.A. Cahill, Appl. Phys. Lett. 66 (1995) 26.
[15] S. Naka, H. Okada, H. Onnagawa, Appl. Phys. Lett. 76 (2000) 197.
[16] F.X. Zang, T.C. Sum, A.C.H. Huan, T.L. Li, W.L. Li, Furong Zhu, Appl. Phys. Lett. 93 (2008) 023309.